Applied Thermal Engineering 31 (2011) 2631–2635

Contents lists available at ScienceDirect

Applied Thermal Engineering

journal homepage: www.elsevier.com/locate/apthermeng

Optimal design of a micro-orifice for constant evaporator superheat in a small cooler

Sangrok Jin [a], Taijong Sung [a], Jongwon Kim [a], TaeWon Seo [b,*]

[a] School of Mechanical and Aerospace Engineering, Seoul National University, Seoul, Republic of Korea
[b] School of Mechanical Engineering, Yeungnam University, Gyeongsan 712749, Republic of Korea

ARTICLE INFO

Article history:
Received 22 March 2011
Accepted 20 April 2011
Available online 29 April 2011

Keywords:
Micro-orifice
Evaporator
Optimal design
Superheat
Small active cooler

ABSTRACT

We present an optimal design for an orifice in a small cooler. The objective of the optimal design is to maintain constant superheat at the outlet of an evaporator while the flow rate and cooling load are changed. Four parameters are chosen for the optimal design: the diameter of the orifice, the aspect ratio between length and diameter, the entrance angle to the orifice, and the surface roughness. R-123 is used as the refrigerant. We perform a simulation to check the sensitivities of each parameter, and we determine the orifice diameter as the most sensitive design parameter among the four parameters to maintain the constant superheat. To find the optimal orifice diameter, experiments are performed on orifices of various diameters. To simulate the vapor-refrigeration cycle, the inlet condition of the orifice upstream flow is fixed at 3 bar and 60 °C. The superheat is measured at the outlet of the orifice while the cooling loads vary by 60, 80, and 100 W and the flow rate varies by 20–70 mL/min. An orifice diameter of 350 μm is selected as the optimal value to keep constant superheat at the evaporator outlet for various flow rates and cooling loads. The resulting optimal orifice design will be used in a small cooler.

1. Introduction

Recently, heat dispersion in portable electronics has become a critical issue [1–3]. Passive air-cooling systems such as fan-fins and heat pipes have cooling capacity limitations. An active cooler based on vapor–compression refrigeration cycles has been proposed as a possible solution. The authors proposed a $50 \times 50\ mm^2$ stack-type active cooler [4] and have recently changed the design of the cooler as shown in Fig. 1(a).

Fig. 1(b) shows refrigerating cycle of the small active cooler which was developed by the authors. Each process of A–D in Fig. 1(b) is matched to characters of device in Fig. 1(a). The compressor (A), that is rotary vane type, compresses refrigerant vapor which is from the evaporator. The refrigerant vapor loses heat and changes to liquid state through the condenser (B) with a heat pipe. Then, the orifice (C) changes the liquid to two-phase vapor in isenthalpic process. The evaporator (D), that has micro lateral gaps, takes the heat from a heat source and supplies saturated vapor (or overheated vapor) to the compressor (A). The whole process is repeated until steady-state.

In the vapor-compression refrigeration cycles which is explained previously, an expansion device is required for the isenthalpic process between the condenser and the evaporator. The expansion device receives liquid state refrigerant from the condenser and converts the refrigerant into two phases. Since wet steam causes poor compressor performance, the expansion device should maintain constant superheat at the outlet of the evaporator by changing the evaporator inlet condition. An orifice is commonly used as the expansion device in small coolers because of its simple structure. Determination of the orifice geometry is very important since the orifice is a passive device. Many researchers suggest analyses on flow characteristics through a micro-orifice [5–9]. Such research is typically focused only on the performance of the orifice. To apply the orifice to a small active cooler, orifice research to find the correlation to the other components that consist of the active cooler such as an evaporator and condenser is required.

We focused on the major role of the orifice to design an active cooler: conservation of constant superheat at the evaporator outlet. Superheat of the evaporator outlet should be maintained as constant for stable operation of a vapor-compression refrigeration cycle. Therefore, the superheat of the evaporator outlet was chosen to establish an objective function for the optimal design of the orifice. We used the evaporator developed in our previous research [10]. The superheat must be maintained in an appropriate range because large superheat decreases the efficiency of an active cooler, and small superheat cannot achieve the refrigeration cycle. In this study, the target superheat was set to 1 °C.

* Corresponding author. Tel.: +82 53 810 2442; fax: +82 2 875 4848.
E-mail addresses: rokjin@rodel.snu.ac.kr (S. Jin), taijsung@rodel.snu.ac.kr (T. Sung), jongkim@snu.ac.kr (J. Kim), taewon_seo@yu.ac.kr (TaeWon Seo).

1359-4311/$ – see front matter © 2011 Elsevier Ltd. All rights reserved.
doi:10.1016/j.applthermaleng.2011.04.032

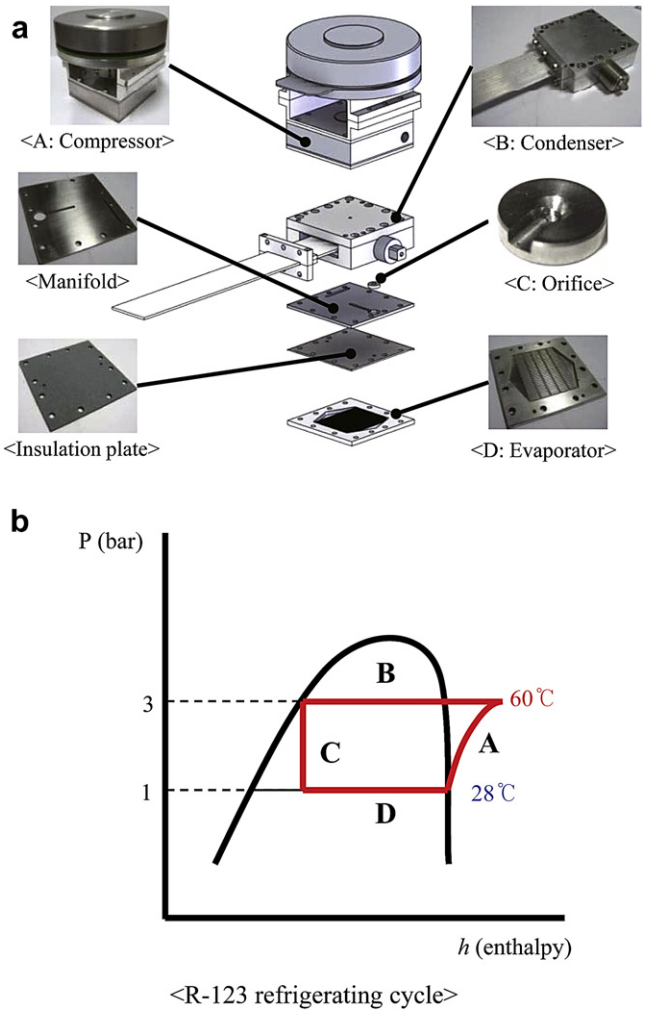

Fig. 1. (a) Concept of stack-type micro-cooler. (b) Refrigerating cycle of the cooler.

The optimal design was performed in two steps. First, the sensitivities of four design parameters (DPs) – diameter, aspect ratio, entrance angle, and roughness – were analyzed by simulation. Then we choose the most sensitive parameter among the four parameters for experimental verification. Experiments were performed by varying the most sensitive parameter while the orifice inlet condition was fixed and the cooling load on the evaporator and the flow rate were changed. The optimal value of the most sensitive parameter was determined by measuring the superheat of the evaporator outlet. The optimal value is also the most robust DP since we considered the variation of the superheat in the objective function.

The rest of the paper is organized as follows. Section 2 defines the optimal design problem according to the design of experiment methodology. Section 3 presents the results of the simulation used to find the most sensitive DP. In Section 4, we describe the optimal DP-based experiments for various conditions. Our conclusions are given in Section 5.

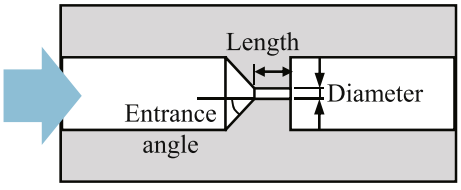

Fig. 2. Cross-section view of the orifice design.

Table 1
DPs and levels.

		Level 1	Level 2	Level 3
A	Diameter	300 μm	350 μm	400 μm
B	Aspect ratio	1.7	2	2.3
C	Entrance angle	40°	45°	50°
D	Roughness	6.3 S	25 S	100 S

2. Problem definition

Our optimal design was performed in two steps: simulation to determine the most sensitive parameter, and experiments to determine the final optimal value. This section describes the objective function, the DP, and constraints for the optimal design.

Before starting to explain the detail procedure, it is important to mention why we perform the optimization process in two steps of simulation and experiment. In our experience, simulation is sometimes not perfectly coincident to the experimental data; especially in phase-change heat transfer problems. In this point of view, we cannot trust the absolute value of the simulation in the expansion device, but we just believe the sensitivity analysis which gives us relative data. We can reduce the design parameters by sensitivity analysis, then we find the final optimal value by small numbers of experiments. By the two-step optimization by simulation and experiment, we can say the optimization procedure becomes efficient and feasible.

2.1. Objective function

The objective of the optimal design is to determine DPs for a constant superheat of 1 °C. We adopted the Nominal-the-Best signal-to-noise (S/N) ratio [11] as the objective function as follows:

$$S/N = -\log\left(\frac{\sum_{i=1}^{n} e_k^2 - S}{n-1}\right), \quad S = \frac{\left(\sum_{i=1}^{n} e_k\right)^2}{n}, \tag{1}$$

where e_i is the difference between the measured superheat and the objective value of 1 °C, and n is the number of simulations or experiments. By introducing the S/N ratio as the objective function, we can find the most robust DP that maintains the superheat near 1 °C.

2.2. Parameters

The four design parameters to be optimized are the diameter, aspect ratio, entrance angle, and roughness. Fig. 2 shows the geometric meaning of each design parameter. The aspect ratio is the ratio of the orifice length to the orifice diameter.

2.3. User condition (noise factor)

There are two noise factors (NFs) that simulate the real operation of the active cooler: the cooling load of the evaporator and the flow

Table 2
Three combinations of NFs.

	NF1	NF2	NF3
Cooling load	60 W	80 W	100 W
Flow rate	30 mL/min	40 mL/min	50 mL/min

Table 3
Simulation results based on orthogonal array $L_9(3^4)$.

Simulation number	Design parameters (levels)				Noise factors			S/N ratio
	A	B	C	D	NF1	NF2	NF3	
					Superheat (°C)			
1	1	1	1	1	1.908	1.924	1.933	38.014
2	1	2	2	2	1.797	1.813	1.801	41.788
3	1	3	3	3	1.866	1.855	1.862	44.849
4	2	1	2	3	1.884	1.901	1.896	40.860
5	2	2	3	1	1.915	1.904	1.891	38.445
6	2	3	1	2	1.925	1.909	1.939	36.367
7	3	1	3	2	1.885	1.900	1.903	40.240
8	3	2	1	3	1.941	1.935	1.907	34.849
9	3	3	2	1	1.905	1.909	1.888	38.939

rate. It should be possible to use the active cooler to cool both the low heat generation device and the high heat generation device. To find a robust solution, cooling loads of 60, 80, and 100 W were applied. The flow rate can be changed during the operation using the compressor power and heat dispersion rate. We used R-123 refrigerant with a flow rate between 20 mL/min and 70 mL/min. By applying the two NFs, we can find a robust solution while the user condition changes.

2.4. Constraints

The inlet condition of orifice upstream flow was fixed at a liquid state at 3 bar and 60 °C. The inner diameter of the pipe (the blue arrow in Fig. 2) was fixed at 2 mm (For interpretation of the references to color in this paragraph, the reader is referred to the web version of this article.).

3. Simulation

As discussed in the previous section, four DPs are to be optimized: the diameter, the aspect ratio, the entrance angle, and the roughness. The objective was to find the most sensitive DP to enhance the objective function among the four DPs. The most sensitive DP was then experimentally analyzed in detail.

3.1. Design of simulation

A simulation to evaluate the sensitivity was performed based on the design of experiment (DOE) methodology [11]. The DOE was performed as follows: i) Choose possible DP candidates at two or three levels. ii) Make the NF combination of extreme user conditions. iii) Design the experiment with an orthogonal array. iv) Determine the optimal value from sensitivity analysis for each DP. In the simulation, we attempted to find only the most sensitive DP among the four DPs.

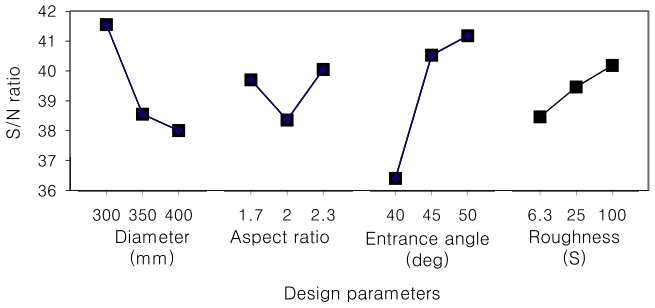

Fig. 4. Sensitivity analyses for each design parameter.

Table 1 shows the possible DP candidates. Three levels of DPs were selected to check the sensitivities for each DP. The cooling load supplied to evaporator and flow rate of the refrigerant through the orifice were considered as NFs. NF combinations were designed as shown in Table 2 to simulate extreme user conditions.

An orthogonal array of $L_9(3^4)$ was used in the simulation as shown on the left side of Table 3. Orthogonal arrays have the advantage that the number of simulations can be reduced. For example, for an analysis of four DPs (as was the case in our research), $3^4 = 81$ simulations are required for each NF in an exhaustive searching method. By using the $L_9(3^4)$ orthogonal array, nine simulations for each NF is enough to check the sensitivity on each DP.

3.2. Performing the simulation

Simulations were performed using ANSYS CFX software (Version 13, ANSYS Inc., Canonsburgh, USA). To calculate the superheat at the evaporator outlet, we simulate the vapor quality at the outlet of the orifice by the ANSYS CFX software. The posture of the simulation is shown in Fig. 3. Then, the enthalpy at the outlet of the evaporator, h_{out}, can be calculated as follows:

$$h_{out} = h_{in} + \frac{Q}{\dot{m}}, \tag{2}$$

where h_{in} is the enthalpy at the outlet of the orifice calculated from the simulated vapor quality, Q is the heat exchange of the refrigerant in the evaporator which is same as the cooling load (note that we assume the housing of the evaporator is well insulated), and $\dot{m}$ is the mass flow rate. The superheat at the outlet of the evaporator can be simply calculated from the resulting h_{out}.

Nine simulations were performed based on the $L_9(3^4)$ orthogonal array, and the resulting superheats are shown in the center of Table 3. The results were analyzed using the S/N ratio.

3.3. Sensitivity analysis

The sensitivity of each DP regardless of NFs was analyzed using the Nominal-the-Best S/N ratio (Eq. (1)). By maximizing the S/N

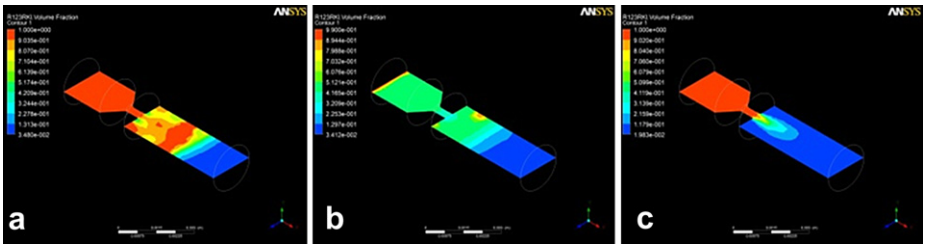

Fig. 3. Result of ANSYS simulation: simulation number 5 (the diameter = 350 μm, the aspect ratio = 2, the entrance angle = 50°, and the surface roughness = 6.3 S. a) NF1 (60 W, 30 mL/min), b) NF2 (80 W, 40 mL/min), c) NF3 (100 W, 50 mL/min).

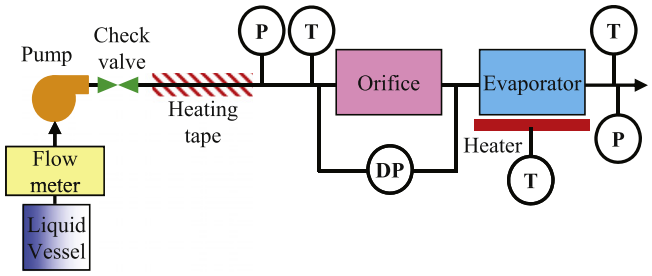

Fig. 5. Schematic diagram of experimental apparatus.

ratio, we obtained the most robust DP that maintained a constant superheat of 1 °C. The *S*/*N* ratio determines how the system performs despite the effects of noise by including the influence of NFs in the denominator [11]. The resulting *S*/*N* ratio is shown on the right side of Table 3. According to the orthogonal array, the *S*/*N* ratio for each level of DP can be calculated. For example, the *S*/*N* ratio of level 2 of B is the average of the *S*/*N* ratio of simulation numbers 2, 5, and 8.

The results of the sensitivity analysis of each DP are shown in Fig. 4. We note that the diameter (A) and the entrance angle (B) have high sensitivity that can be expressed by the variation between the maximum and minimum value of the *S*/*N* ratio. In contrast, the other two DPs do not have high sensitivity with respect to the objective function.

To increase the objective efficiently, it is important to see the shape of sensitivity curve of the two sensitive DPs. In the curve of the entrance angle, the sensitivity is not high in the high *S*/*N* ratio region, which means the objective function reaches almost the maximum around 45 and 50°; thus we cannot expect to increase the objective sharply by increasing the entrance angle. In the curve of the diameter, the sensitivity is high in the high *S*/*N* ratio region. Therefore we can efficiently increase the objective function by varying the sensitive DP in the high *S*/*N* ratio region; i.e., the diameter. In terms of manufacturing cost, it is efficient to reduce the number of experiments. Therefore, we performed the optimization experiment only on the diameter.

4. Experiments

4.1. Set-up of experiment

A diagram of the experimental apparatus is shown in Fig. 5. A liquid volumetric pump (KPV-22-SF-S, Cheon-Sei Industries, Korea) was used to draw R-123 refrigerant from a liquid vessel. A float flow meter (custom made, KITS, Korea) for liquid R-123 measured the volume flow rate. Heating tape regulated the experimental orifice inlet conditions. A pressure sensor (Model 206, Setra Systems, Boxborough, USA), differential pressure transducers (Model 230, Setra System), and a type-K thermocouple were used to measure the pressures and temperatures of the refrigerant at the inlet and the outlet of the orifice. Cartridge heaters were adhered under the evaporator to apply the cooling load. A direct current (DC) power supply provided constant power to the cartridge heaters to achieve various cooling loads. A pressure transducer and thermocouple measured the pressure and temperature of the refrigerant, respectively, at the outlet of the evaporator. All experimental equipment was insulated using expanded polystyrene tubes and polyether ether ketone (PEEK) housings.

Fig. 6(a) shows the manufactured orifice samples. The entrance angle is 45° and the aspect ratio is 2. Four orifice samples were manufactured with diameters of 300, 350, 400, and 450 μm. A micro-evaporator with a lateral gap, shown in Fig. 6(b), was installed after the orifice sample [10]. During the experiments, the inlet condition to the orifice was maintained at 3 bar and 60 °C by the heating tape. Cartridge heaters under the evaporator supplied cooling loads of 60, 80, and 100 W. The volumetric pump controlled the flow rate in the range of 20–70 mL/min for each orifice sample. Note the two varying conditions of the cooling loads and the flow rate simulate the user condition to find a robust diameter of the orifice.

The calculation for the superheat at the evaporator outlet was made as follows. The saturation temperature was derived from measured pressure at the evaporator outlet. Then, the superheat was determined by subtracting the saturation temperature from the measured temperature at the evaporator outlet. All data were measured at the steady-state condition. Some data at low flow rate and high cooling load resulted in inconsistent results; thus, we did not consider these data in the analysis.

4.2. Results

Before we discuss the superheat, we would like to explain measured pressure drop and flow rate. In theory, the pressure drop and the flow rate have strong correlation in single phase flow; however, the pressure drop maintains constant while the flow rate affects the vapor quality in two-phase flow. In our experiments, the pressure drop is measured by constant in the region of interest. And the flow rate turns out to be proportional to the vapor quality which is going to be used to calculate the superheat as explained in Section 4.1.

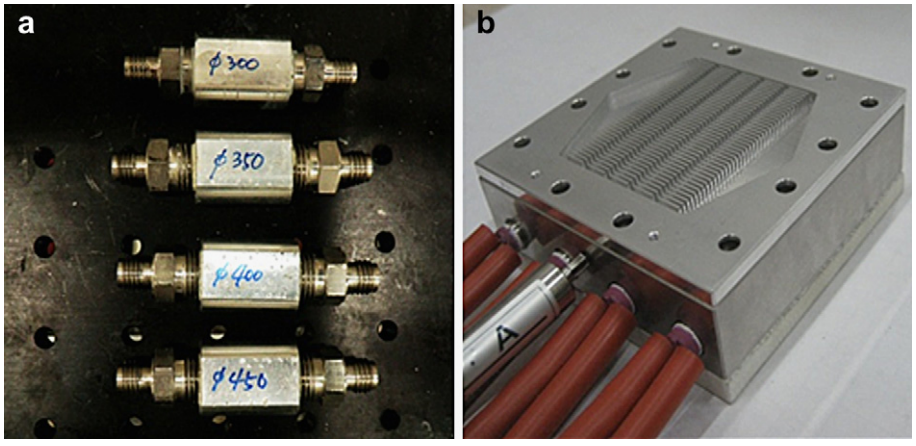

Fig. 6. Photo of (a) orifice samples, and (b) micro-evaporator with cartridge heaters.

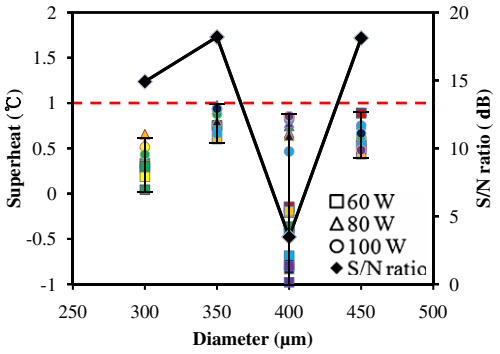

Fig. 7. Superheat of refrigerant at the evaporator outlet and *S*/*N* ratio for each orifice diameter: red dotted line denotes the objective superheat of 1 °C. The shape of the point denotes different cooling loads: the square, triangle, and circle mean 60 W, 80 W, and 100 W, respectively. The color of the point denotes different flow rates: red, orange, yellow, green, blue, navy, and purple indicates 25, 30, 35, 40, 50, 60, and 70 mL/min, respectively. (For interpretation of the references to color in this figure legend, the reader is referred to the web version of this article.)

The superheat at the evaporator outlet and the *S*/*N* ratio for each flow rate and cooling load are shown in Fig. 7. The 350 μm orifice had the largest *S*/*N* ratio of 18.2 dB, and the 450 μm orifice had the second largest *S*/*N* ratio of 18.1 dB. Note that there is no significant difference between the two diameters. However, in the design problem based on the Nominal-the-Best *S*/*N* ratio, we should consider the error between the measured value and the objective value of 1 °C since the largest *S*/*N* ratio only guarantees the smallest variation. In other words, the *S*/*N* ratio guarantees the robustness of the DP and the error guarantees the performance. In the error analysis, the 350 μm orifice showed an error of 0.19 °C and the 450 μm orifice showed an error of 0.40 °C. Therefore, 350 μm was determined to be the optimal orifice diameter to ensure both robustness and performance.

We note that the 300 μm orifice had a higher *S*/*N* ratio than the *S*/*N* ratio of the 350 μm orifice in the simulation, and 350 μm was determined to be the final optimal DP in the experiments. We think that the incoincidence between simulation and experiment is from some factors that the simulation cannot simulate such as flow resistance and the correlation between the orifice and the evaporator. Second, the superheat of the 400 μm orifice at 60 W resulted in temperature below the saturation point in the experiment. This is very interesting since the 450 μm orifice resulted in positive superheat. We suspect that this phenomenon is due to a correlation effect between the orifice diameter and the cooling load. Research on this correlation could be an interesting topic for future work.

5. Conclusions

We conducted an optimal design of the geometric parameters of an orifice for constant superheat at the evaporator outlet regardless of variations in flow rate and cooling load. An objective function that considered the deviation of the superheat, four DPs of orifice geometry, user conditions of various cooling loads and flow rates, and a constraint on the inlet condition was defined. Sensitivity analysis by simulation was performed and we determined the diameter of the orifice as the most sensitive DP to maintain the constant evaporator outlet superheat. Experiments were conducted on various diameters to find the optimal diameter. The cooling load and the flow rate were varied in the experiment. 350 μm was determined to be the optimal orifice diameter, with the largest *S*/*N* ratio of 18.2 dB and the smallest difference of 0.19° to the objective superheat of 1°. The resulting orifice diameter of 350 μm will be applied to develop an active micro-cooler based on a vapor-compression refrigeration cycle.

We believe the two-step optimization procedure of simulation and experiment can be adopted to other design of micro-cooler for both efficiency and feasibility. Also, our approach to use the superheat instead of the vapor quality has an advantage of simplicity in measurement. Additionally, the resulting superheat can be used to construct the whole refrigeration cycle of a micro-cooler.

Acknowledgements

This work is supported by the Yeungnam University research grants in 2010.

References

[1] R.J. McGlen, R. Jachuck, S. Lin, Integrated thermal management techniques for high power electronic devices, Applied Thermal Engineering 24 (2004) 1143–1156.
[2] A.G. Agwu Nnanna, Application of refrigeration system in electronics cooling, Applied Thermal Engineering 26 (2006) 18–27.
[3] Z. Wu, R. Du, Design and experimental study of a miniature vapor compression refrigeration system for electronics cooling, Applied Thermal Engineering 31 (2011) 385–390.
[4] T. Sung, D. Oh, T. Seo, J. Kim, Optimal design of a micro evaporator to maximize heat transfer coefficient, in: Asian Symposium for Precision Engineering and Nanotechnology (2007) pp. 63–66.
[5] Y. Kim, D.L. O'Neal, A semi-empirical model of two-phase flow of Refrigerant-134a through short tube orifices, Experimental Thermal and Fluid Science 9 (1994) 426–435.
[6] Y. Kim, D.L. O'Neal, Two-phase flow of R-22 through short-tube orifices, ASHRAE Transactions 100 (1994) 323–334.
[7] R. Diener, J. Schmidt, Sizing of throttling device for gas/liquid two-phase flow part 2: control valves, orifices, and nozzles, Process Safety Progress 24 (1) (2005) 29–37.
[8] X. Tu, P.S. Hrnjak, C.W. Bullard, Refrigerant 134a liquid flow through micro-scale short tube orifices with/without phase change, Experimental Thermal and Fluid Science 30 (2006) 253–262.
[9] K. Ramamurthi, K. Nandakumar, Characteristics of flow through small sharp-edged cylindrical orifices, Flow Measurement and Instrumentation 10 (1999) 133–143.
[10] T. Sung, D. Oh, S. Jin, T. Seo, J. Kim, Optimal design of a micro evaporator with lateral gaps, Applied Thermal Engineering 29 (2009) 2921–2926.
[11] G. Taguchi, Taguchi on Robust Technology Development: Bringing Quality Engineering Upstream. ASME Press, 1993.